Journal of Organometallic Chemistry, 322 (1987) 331–350
Elsevier Sequoia S.A., Lausanne – Printed in The Netherlands

NATURE OF THE HYDROGEN BRIDGE IN TRANSITION METAL COMPLEXES

I. MOLECULAR ORBITAL CALCULATIONS OF BINUCLEAR CARBONYLS OF Cr, Mo Fe AND Ni WITH SINGLE HYDROGEN BRIDGES

BOGUSŁAWA JEŻOWSKA-TRZEBIATOWSKA* and BARBARA NISSEN-SOBOCIŃSKA

Institute for Low Temperature and Structure Research, Polish Academy of Sciences, Plac Katedralny 1, 50-950 Wrocław (Poland)

and

Institute of Chemistry, Wrocław University, F. Joliot-Curie 14, 50-383 Wrocław (Poland)

(Received September 28th, 1986)

Summary

Determination of the electronic structure was performed by the parameter-free Fenske–Hall method for the complexes $[(CO)_5M–H–M(CO)_5]^-$ with D_{4h}, C_{2v} and C_2 symmetries (where M = Cr, Mo) as well as for the complex $[(CO)_3Ni–H–Ni(CO)_3]^-$ with C_{2v} and D_{3h} symmetries and for the complex $[(CO)_4Fe–H–Fe(CO)_4]^+$ with a D_{3h} symmetry.

The character and stability of the metal–hydrogen–metal bridge bond in each of these complexes was compared. The effect of lowering the symmetry on the electronic structure of these complexes is also discussed. The influence of the bridging hydrogen atom on terminal ligands, i.e. its *cis* effect, was characterized.

Introduction

Our interest in the electronic structure of bridged binuclear transition metal complexes also prompted us to investigate the molecular structure of several series of hydrogen-bonded metal systems by use of quantum chemistry methods. At present we know of a fairly large group of transition metal complexes containing metal–hydrogen–metal bridge bonds (M–H–M) the structures of which were determined by X-ray and neutron diffraction methods [1]. These can be dimers or clusters of several atoms in the molecule containing single, double, triple or even quadruple hydrogen bridges, as well as mixed bridges. In addition to hydrogen atoms the bridging ligands can be phosphines, chlorides, hydroxyl and carbonyl groups.

0022-328X/87/$03.50

An analogous M–H–M bond described as an "electron-deficient, 3-center-2-electron bond" occurs in Group IIIA compounds viz. in boranes and the dimethyl aluminium hydride dimer. The diborane $H_2B\begin{smallmatrix}H\\ \diagup\diagdown\\ H\end{smallmatrix}BH_2$ is the simplest of the group of borane clusters and its electronic structure has been characterized by many, more- or less-advanced methods [2]. A common result of these calculations is that the B–H–B bridge is exclusively covalent and that the boron atoms interact with one another mainly through the hydrogen bridge. On the other hand, ab initio SCF calculations [3], and our own calculations by the Fenske–Hall method, showed that for $(CH_3)_2Al\begin{smallmatrix}H\\ \diagup\diagdown\\ H\end{smallmatrix}Al(CH_3)_2$ [4] a fairly large contribution of ionic character to the Al–H–Al bridge bond was present which is manifested by a large negative charge localized on the hydrogen atoms and a large positive charge localized on the metal atoms.

Common properties of the electronic structures of the $B\begin{smallmatrix}H\\ \diagup\diagdown\\ H\end{smallmatrix}B$ and $Al\begin{smallmatrix}H\\ \diagup\diagdown\\ H\end{smallmatrix}Al$ cores are; (i) low delocalization of the atomic orbitals of the bridging hydrogen, (ii) fairly high stability of the hydrogen bridges and (iii) very slight direct B–B and Al–Al bonds.

Our studies were directed only at transition metal carbonyls containing a single hydrogen bridge. Not many such compounds have been known till now, and include, chromium, molybdenum and tungsten carbonyls such as $[(CO)_5M–H–M(CO)_5]^-$ or $[(CO)_5M–H–M'(CO)_5]^-$ where M, M' = Cr, Mo, W [5]. Similar complexes are formed by nickel. A crystallographic structure is known for

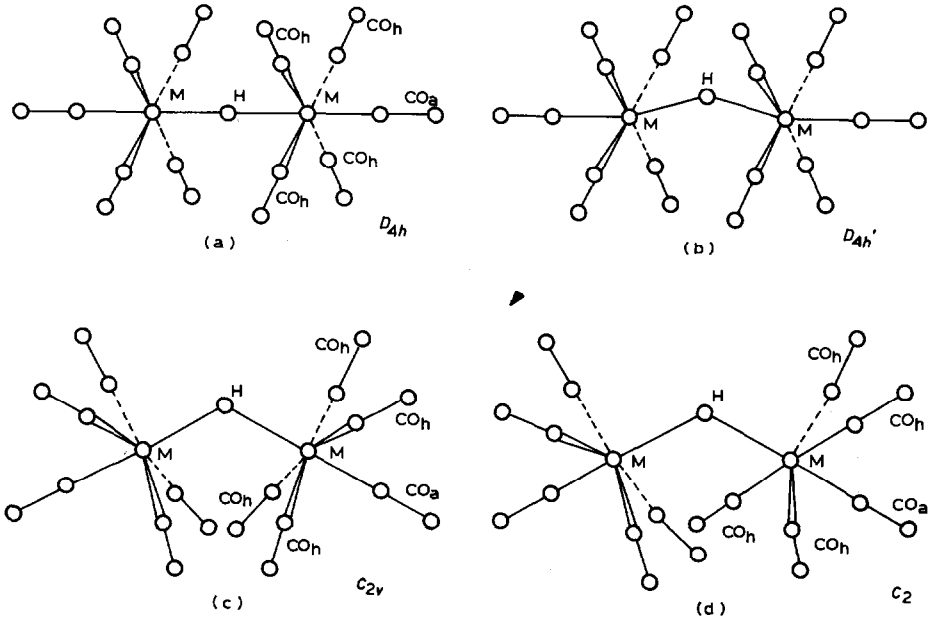

Fig. 1. Possible conformations of the $[(CO)_5M–H–M(CO)_5]$ anions.

$[(CO)_3Ni–H–Ni(CO)_3]^-$ [6]. Iron and niobum form complexes with a mixed core, $(\pi\text{-}C_5H_5)_2(CO)Nb–H–Fe(CO)_4$, whose crystallographic structure has also been determined [7].

The complexes of the type $[(CO)_5M–H–M(CO)_5]^-$ belong to the complexes first discovered to contain the M–H–M bridge bond [8]. Initially it was found that the M–H–M bond in these complexes is linear and their symmetry corresponds to the D_{4h} point group [8,9]. However, further detailed X-ray and neutron diffraction studies showed that the M–H–M angle depends to a large extent on the type of cation bound to the $[(CO)_5M–H–M(CO)_5]^-$ anion in the crystal lattice [10]. The M–H–M angle varies over a fairly broad range (from 120° to 180°), indicating that this bond is very flexible. For the linear M–H–M bond the two $M(CO)_5$ moieties are in eclipsed positions, whereas for the angular M–H–M bond the relative orientation of these groups depends on the value of the M–H–M angle. A decrease in the bridge bond angle increases the displacement angle between the $M(CO)_5$ moieties. It is interesting to note how these geometrical changes affect the electronic structure of the $[(CO)_5M–H–M(CO)_5]^-$ anions. To study this problem, we performed calculations for chromium and molybdenum complexes for the eclipsed conformation having a linear bridge with D_{4h} symmetry, eclipsed conformation having a bent bridge with C_{2v} symmetry or a staggered conformation having a bent bridge with C_2 symmetry (Fig. 1a, 1c, 1d). The coordinate systems on the atoms assumed for calculations for these complexes are presented in Fig. 2.

In all the structures of the known $[(CO)_5M–H–M(CO)_5]^-$ anions, the metal–carbon bonds in axial positions ($M–C_a$) have been found to have been shortened with respect to other metal–carbon bonds ($M–C_h$). This indicates that the carbonyl groups in axial positions (CO_a) are better π-acceptors than those in the equatorial positions (CO_h) hence the $M–C_a$ bonds are stronger than $M–C_h$ bonds. The values of Cotton–Kraihanzel force constants calculated from the IR spectra for $[(CO)_5Cr–H–Cr(CO)_5]^-$ also indicate that the CO_a groups are more strongly bound to the Cr atoms than the CO_h groups [11]. This has been confirmed experimentally, in that the CO_h groups are more labile in substitution reactions [11,12,13]. To test this effect, we assumed the same bond lengths for $M–C_h$ and $M–C_a$.

In the case of the M–H–M bonds for the systems with single hydrogen bridges it

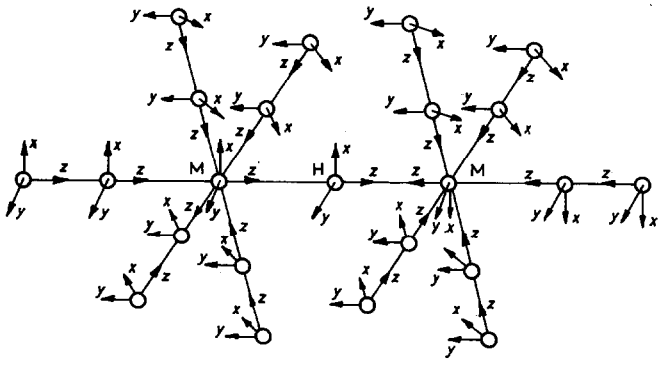

Fig. 2. Coordinate systems assumed in calculations for the $[(CO)_5M–H–M(CO)_5]^-$ anions.

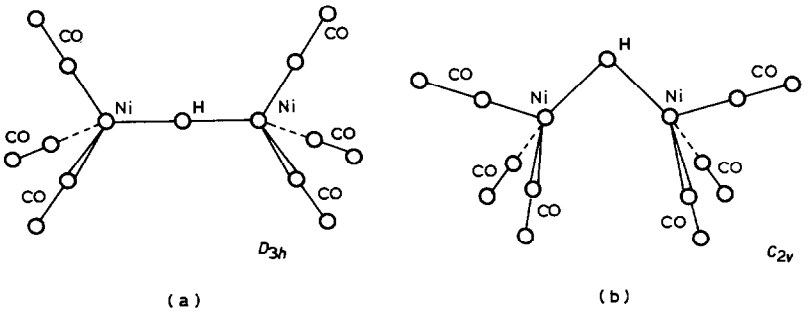

Fig. 3. Conformations of the $[(CO)_3Ni-H-Ni(CO)_3]^-$ anion assumed in calculations.

is also essential to know whether the bridging hydrogen atom is equidistant from both metal atoms, as found for most crystallographic structures, or whether it is only at a statistically equal distance. Some recent work indicates that there is a double minimum in the potential energy of the M–H–M bond. For instance, the neutron diffraction structure of the $[NEt_4]^+$ $[W_2(\mu\text{-H})(CO)_{10}]^-$ complex determined at 14 K is characterized by high asymmetry of the W–H–W bond [1a]. Double potential energy minima are also found in the IR spectra of the $[(CO)_5M-H-M(CO)_5]^-$ anions at low temperatures, corresponding to asymmetric M–H stretch [14].

After determination of the precise neutron diffraction structures [1a,1b,10c,10d, 10e,10g,10h] it was also shown that in $[(CO)_5M-H-M(CO)_5]^-$ anions with D_{4h} symmetry, the hydrogen atom is slightly shifted with respect to the complex symmetry centre, along the axis normal to the straight line linking the metal atoms (Fig. 1b). Thus the M–H–M bond is by its very nature inherently bent [1b]. In our calculations, however, we assumed that the M–H–M bond was perfectly linear. This assumption results from the limitations of the method applied, since any allowance for the asymmetry of the M–H–M bond or for the "natural" bend of the linear M–H–M bond causes changes in the results contained within experimental error.

The Ni–H–Ni bond in the nickel complex has been found to be bent and the mononuclear $Ni(CO)_3$ moieties are eclipsed [6]. We performed calculations for

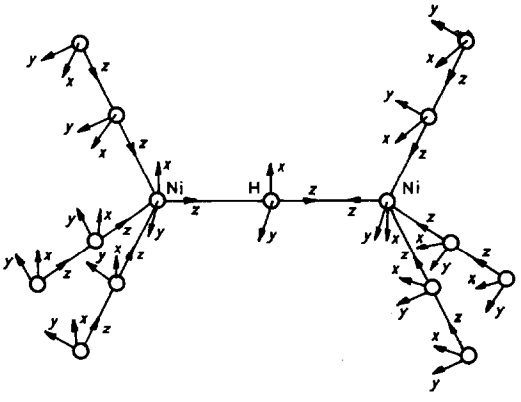

Fig. 4. Coordinate systems assumed in calculations for the $[(CO)_3Ni-H-Ni(CO)_3]^-$ anion.

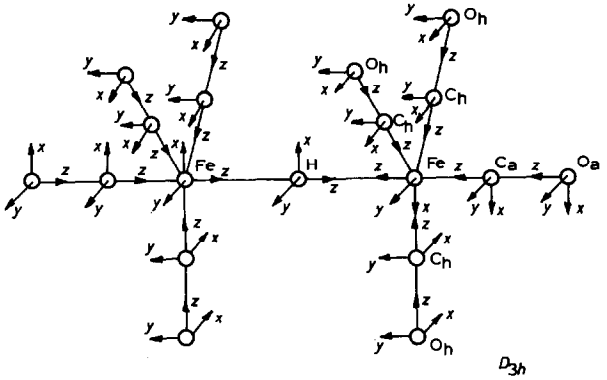

Fig. 5. Coordinate systems assumed in calculations for the $[(CO)_4Fe–H–Fe(CO)_4]^-$ anion.

$[(CO)_3Ni–H–Ni(CO)_3]^-$ with D_{3h} and C_{2v} symmetries (Fig. 3, 4) and also for a hypothetical $[(CO)_4Fe–H–Fe(CO)_4]^-$ complex with D_{3h} symmetry (Fig. 5).

The basis for the selection of the structural parameters for the chromium anion was the neutron diffraction structure of $[K(C_{18}H_{36}N_2O_6)]^+$ $[Cr_2(\mu\text{-}H)(CO)_{10}]^-$ [10h] and for the molybdenum anion the neutron diffraction structure of $[K(C_{18}H_{36}N_2O_6)]^+$ $[Mo_2(\mu\text{-}H)(CO)_{10}]^-$ [10i]. In these compounds the $[M_2(\mu\text{-}H)(CO)_{10}]^-$ anions have C_2 symmetry. The M–H–M angle for the chromium anion is about 145° and the staggering angle of the mononuclear $M(CO)_5$ moieties is about 20°, whereas for the molybdenum anion these angles are 127° and 45° respectively. These values were assumed in our calculations for systems with C_{2v} and C_2 symmetries.

Thus the following bond lengths were assumed for the chromium complex: Cr–Cr 3.40 Å for D_{4h} symmetry; Cr–Cr 3.30 Å for C_{2v} and C_2 symmetries; Cr–H 1.70, Cr–C 1.88, C–O 1.15 Å; and for the molybdenum complex: Mo–Mo 3.80 Å for the D_{4h} symmetry, Mo–Mo 3.40 Å for the C_{2v} and C_2 symmetries, Mo–H 1.90, Mo–C 1.99, C–O 1.14 Å. According to neutron diffraction data for $[(Ph_3P)_2N]^+$ $[Ni_2(\mu\text{-}H)(CO)_6]^-$ [6] we assumed the following bond lengths for the nickel complex: Ni–Ni 3.40 Å for D_{3h} symmetry, Ni–H 1.70, Ni–C 1.73, C–O 1.17 Å and the angles: Ni–H–Ni 115, C–Ni–C 114°. The structural parameters for the iron complex were assumed on the basis of the crystallographic structure of $(\pi\text{-}C_5H_5)_2(CO)Nb–H–Fe(CO)_4$ [7]. Thus the following bond lengths were assumed: Fe–Fe 3.22, Fe–H 1.61, $Fe–C_a = Fe–C_h = 1.79$, $C_a–O_a = C_h–O_h = 1.15$ Å.

All calculations were performed by the parameter-free Fenske–Hall method [15], suitably optimized functions of the following types were used for the calculations: $1s$, $2s$, $2p$ of the C and O atoms, $1s$ of the H atom and $1s$, $2s$,$2p$,…,$(n-1)d$, ns, np of the given metal atoms.

Results and discussion

1. Characteristics of the electronic structure of complexes with linear hydrogen bridges

Electronic structures of complexes with linear hydrogen bridges of the type $[(CO)_5M–H–M(CO)_5]^-$ where M = Cr, Mo with D_{4h} symmetry as well as $[(CO)_3Ni–H–Ni(CO)_3]^-$ and $[(CO)_4Fe–H–Fe(CO)_4]^-$ complexes with D_{3h} sym-

metry are very similar in (i) the order and energy of the molecular levels, and (ii) their qualitative and quantitative compositions. The order of the filled energy levels of these complexes determined on the basis of the valence atomic orbitals of the metal, carbon, oxygen and hydrogen can be generalized in the following way:

(1) energy levels with exclusively σMO character of the CO groups,

(2) energy levels with exclusively π^bMO character of the CO groups,

(3) energy levels corresponding to bonding interactions of the MOs of the CO groups with the d, p and s (only for Ni) AOs of metal atoms i.e. δCO–M interactions,

(4) energy level of the M–H–M bridge bond,

(5) energy levels corresponding to bonding interactions of the unfilled π^aMOs of the CO groups with the dAOs of metal atoms, i.e. $d\mathrm{M} \rightarrow \pi^a(\mathrm{CO})$ interactions.

Tables 1, 4, 7 and 9 show selected molecular orbitals for the above-mentioned complexes and in Fig. 6 a correlation of the respective energy levels is shown. A characteristic feature of all these systems is that the 1s orbital of the bridging hydrogen atom makes a considerable contribution to the formation of one bonding

TABLE 1

ENERGIES AND COMPOSITIONS OF THE HIGHEST OCCUPIED MOLECULAR LEVELS OF $[(CO)_5Cr\text{–}H\text{–}Cr(CO)_5]^-$ WITH D_{4h} SYMMETRY

MO	Energy (eV)	Largest contributions of the valence atomic orbitals (%)					
$8a_{2u}$ LUMO	1.64	$p_y(C_h)$	37	$3d_{z^2}$(Cr)	22	$p_y(O_h)$	21
$7e_g$ HOMO	−3.22	$3d_{xz}$(Cr) [a] $3d_{yz}$	58	$p_y(O_h)$	13	$p_y(C_h)$	12
$7e_u$	−3.50	$3d_{xz}$(Cr) [a] $3d_{yz}$	55	$p_y(O_h)$	15	$p_y(C_h)$	15
$2b_{2u}$	−3.96	$3_{dx^2-y^2}$(Cr)	51	$p_x(O_h)$	26	$p_x(C_h)$	22
$2b_{1g}$	−4.01	$3d_{x^2-y^2}$(Cr)	50	$p_x(O_h)$	26	$p_x(C_h)$	23
$8a_{1g}$	−6.49	s(H)	78	$3d_{z^2}$(Cr)	7	$p_z(C_a)$	3
$6e_g$	−10.50	$p_z(C_h)$	37	$s(C_h)$	26	p_x(Cr) p_y	12
$6e_u$	−10.52	$p_z(C_h)$	37	$p_z(O_h)$	17	p_x(Cr) p_y	11
$7a_{2u}$	−11.58	$p_z(C_a)$	26	$3d_{z^2}$(Cr)	25	$p_z(O_a)$	19
$7a_{1g}$	−11.82	$3d_{z^2}$(Cr)	29	$p_z(C_a)$	24	$p_z(O_a)$	18
$4b_{1u}$	−12.22	$3d_{xy}$(Cr)	36	$p_z(C_h)$	26	$p_z(O_h)$	22
$4b_{2g}$	−12.23	$3d_{xy}$(Cr)	36	$p_z(C_h)$	26	$p_z(O_h)$	23
$6a_{1g}$	−14.24	$p_z(O_h)$	38	$p_z(C_h)$	29	s(Cr)	7
$6a_{2u}$	−14.28	$p_z(O_h)$	37	$p_z(C_h)$	28	s(Cr)	8
$5e_g$	−15.46	$p_x(O_a)$ [a] p_y	53	$p_x(C_a)$ [a] p_y	28	$p_y(O_h)$	12
$5e_u$	−15.49	$p_x(O_a)$ [a] p_y	56	$p_x(C_a)$ [a] p_y	31	$p_y(O_h)$	6
$1a_{1u}$	−15.69	$p_x(O_h)$	71	$p_x(C_h)$	29		
$1a_{2g}$	−15.70	$p_x(O_h)$	70	$p_x(C_h)$	30		
$3b_{1u}$	−15.83	$p_y(O_h)$	67	$p_y(C_h)$	33		
$3b_{2g}$	−15.97	$p_y(O_h)$	65	$p_y(C_h)$	35		

[a] Doubly degenerated molecular level.

TABLE 2

ENERGIES AND COMPOSITIONS OF HIGHEST OCCUPIED MOLECULAR LEVELS OF $[(CO)_5Cr–H–Cr(CO)_5]^-$ WITH C_{2v} SYMMETRY

MO	Energy (eV)	Largest contributions of the valence atomic orbitals (%)					
$17b_1$ LUMO	2.41	$3d_{z^2}$(Cr)	26	$p_y(C_h)$	18	p_z(Cr)	17
$16b_1$ HOMO	−2.82	$3d_{xz}$(Cr)	46	$3d_{z^2}$(Cr)	11	$p_y(C_h)$	11
$12a_2$	−2.83	$3d_{yz}$(Cr)	55	$p_x(C_a)$	8	$p_x(O_a)$	8
$15b_1$	−3.76	$3d_{x^2-y^2}$(Cr)	51	$p_x(O_h)$	25	$p_x(C_h)$	9
$12b_2$	−3.78	$3d_{yz}$(Cr)	47	$p_y(C_h)$	12	$p_y(O_h)$	9
$17a_1$	−3.78	$3d_{xz}$(Cr)	24	$3d_{x^2-y^2}$(Cr)	19	$3d_{z^2}$(Cr)	10
$16a_1$	−4.19	$3d_{x^2-y^2}$(Cr)	31	$p_x(O_h)$	20	$3d_{xz}$(Cr)	15
$15a_1$	−6.44	s(H)	71	$3d_{z^2}$(Cr)	7	$p_z(C_a)$	5

molecular orbital. Such a slight delocalization of the atomic orbitals of the bridging hydrogen atoms is also typical for the other carbonyl complexes examined by us. Therefore, in this respect the M–H–M bond in these complexes resembles the B–H–B and Al–H–Al bonds found in $H_2B\langle^{H}_{H}\rangle BH_2$ and $(CH_3)_2Al\langle^{H}_{H}\rangle Al(CH_3)_2$, respectively.

The bridge molecular orbitals, i.e. the $8a_{1g}$ orbital for the chromium and molybdenum complexes, the $5a_1$ orbital for the nickel complex, and the $8a_1$ orbital for the iron complex are delocalized over the entire molecule (Tables 1, 4, 7, 9). In addition to the atomic orbitals of metal and hydrogen, these molecular orbitals are also formed by a contribution from the atomic orbitals of the terminal ligands (mainly the CO_a groups). However, the largest contribution to the formation of the bridge molecular orbitals is provided by the atomic orbitals of hydrogen, which is about 70% for the iron and nickel complexes, while for the chromium and molybdenum complexes it amounts to about 50%.

The energy difference between the last filled orbital (HOMO) and the bridge orbital, i.e. $\Delta E_{HOMO,MO(M-H-M)}$ can be used as a measure of the M–H–M bond stability for a given complex. The energy difference values are very similar for the

TABLE 3

ENERGIES AND COMPOSITIONS OF HIGHEST OCCUPIED MOLECULAR LEVELS OF $[(CO)_5Cr–H–Cr(CO)_5]^-$ WITH C_2 SYMMETRY

MO	Energy (eV)	Largest contributions of the valence atomic orbitals (%)					
29*a* LUMO	2.07	$p_y(C_h)$	30	$3d_{z^2}$(Cr)	22	s(Cr)	16
28*b* HOMO	−2.95	$3d_{yz}$(Cr)	29	$3d_{xz}$(Cr)	20	$p_y(C_h)$	7
29*a*	−2.90	$3d_{xz}$(Cr)	26	$3d_{yz}$(Cr)	26	$p_y(O_h)$	8
27*b*	−3.53	$3d_{yz}$(Cr)	43	$3d_{xy}$(Cr)	8	$p_y(O_h)$	7
28*a*	−3.61	$3d_{xz}$(Cr)	26	$3d_{x^2-y^2}$(Cr)	14	$3d_{z^2}$(Cr)	10
26*b*	−3.97	$3d_{x^2-y^2}$(Cr)	43	$p_x(O_h)$	24	$p_x(C_h)$	12
27*a*	−4.05	$3d_{x^2-y^2}$(Cr)	28	$p_x(O_h)$	22	$3d_{xz}$(Cr)	13
26*a*	−6.37	s(H)	71	$3d_{z^2}$(Cr)	7	$s(C_a)$	3

TABLE 4

ENERGIES AND COMPOSITIONS OF HIGHEST OCCUPIED MOLECULAR LEVELS OF $[(CO)_5Mo–H–Mo(CO)_5]^-$ WITH D_{4h} SYMMETRY

MO	Energy (eV)	Largest contributions of the valence atomic orbitals (%)					
$8a_{2u}$ LUMO	−0.17	$4d_{z^2}$(Mo)	30	$p_y(C_h)$	29	p_z(Mo)	20
$7e_g$ HOMO	−2.47	$4d_{xz}$(Mo) [a] $4d_{yz}$	57	$p_y(C_h)$	14	$p_y(O_h)$	12
$7e_u$	−2.59	$4d_{xz}$(Mo) [a] $4d_{yz}$	54	$p_y(C_h)$	17	$p_y(O_h)$	14
$2b_{2u}$	−3.18	$4d_{x^2-y^2}$(Mo)	49	$p_x(C_h)$	26	$p_x(O_h)$	24
$2b_{1g}$	−3.22	$4d_{x^2-y^2}$(Mo)	49	$p_x(C_h)$	26	$p_x(O_h)$	25
$8a_{1g}$	−6.99	s(H)	67	p_z(Mo)	13	$4d_{z^2}$(Mo)	12
$7a_{1g}$	−11.86	$p_z(C_a)$	24	$4d_{z^2}$(Mo)	23	$p_z(O_a)$	17
$6e_u$	−11.94	$p_z(C_h)$	33	$p_z(O_h)$	20	p_x(Mo) [a] p_y	20
$4b_{2g}$	−11.94	$4d_{xy}$(Mo)	35	$p_z(C_h)$	27	$p_z(O_h)$	20
$4b_{1u}$	−11.96	$4d_{xy}$(Mo)	35	$p_z(C_h)$	27	$p_z(O_h)$	20
$7a_{2u}$	−12.00	$4d_{z^2}$(Mo)	19	$p_z(C_a)$	19	$s(C_a)$	14
$6e_g$	−12.14	$p_z(C_h)$	32	$p_z(O_h)$	21	p_x(Mo) [a] p_y	20
$6a_{1g}$	−14.37	$p_z(O_h)$	34	$p_z(C_h)$	26	s(Mo)	10
$6a_{2u}$	−14.41	$p_z(O_h)$	36	$p_z(C_h)$	26	s(Mo)	11
$5e_g$	−15.67	$p_x(O_a)$ [a] p_y	50	$p_x(C_a)$ [a] p_y	25	$p_y(O_h)$	17
$5e_u$	−15.71	$p_x(O_a)$ [a] p_y	55	$p_x(C_a)$ [a] p_y	28	$p_y(O_h)$	10
$1a_{1u}$	−15.79	$p_x(O_h)$	71	$p_x(C_h)$	29		
$1a_{2g}$	−15.79	$p_x(O_h)$	70	$p_x(C_h)$	30		
$3b_{1u}$	−15.93	$p_y(O_h)$	68	$p_y(C_h)$	32		
$3b_{2g}$	−16.05	$p_y(O_h)$	66	$p_y(C_h)$	34		

[a] Doubly degenerated molecular level

TABLE 5

ENERGIES AND COMPOSITIONS OF HIGHEST OCCUPIED MOLECULAR LEVELS OF $[(CO)_5Mo–H–Mo(CO)_5]^-$ WITH C_{2v} SYMMETRY

MO	Energy (eV)	Largest contributions of the valence atomic orbitals (%)					
$13b_2$ LUMO	1.36	$p_y(C_h)$	56	$4d_{yz}$(Mo)	13	$p_y(O_h)$	12
$12a_2$ HOMO	1.02	$p_y(C_h)$	42	$4d_{xy}$(Mo)	9	$p_y(O_h)$	7
$16b_1$	−0.75	$p_y(C_h)$	43	$4d_{xz}$(Mo)	18	$p_y(O_h)$	11
$15b_1$	−2.57	$4d_{x^2-y^2}$(Mo)	54	$p_x(O_h)$	20	$p_x(C_h)$	13
$11a_2$	−3.30	$4d_{yz}$(Mo)	42	$p_y(C_h)$	22	$p_x(O_a)$	8
$14b_1$	−3.45	p_yC_h	31	$4d_{xz}$(Mo)	22	$4d_{z^2}$(Mo)	18
$17a_1$	−3.53	$4d_{x^2-y^2}$(Mo)	32	$p_x(C_h)$	16	$4d_{z^2}$(Mo)	10
$12b_2$	−3.70	$4d_{yz}$(Mo)	30	$p_y(C_h)$	27	$4d_{xy}$(Mo)	10
$16a_1$	−4.06	$p_y(C_h)$	20	$4d_{xz}$(Mo)	16	$4d_{z^2}$(Mo)	12
$15a_1$	−6.48	s(H)	65	p_z(Mo)	10	$4d_{z^2}$(Mo)	7

TABLE 6

ENERGIES AND COMPOSITIONS OF HIGHEST OCCUPIED MOLECULAR LEVELS OF $[(CO)_5Mo–H–Mo(CO)_5]^-$ WITH C_2 SYMMETRY

MO	Energy (eV)	Largest contributions of the valence atomic orbitals (%)					
29*b* LUMO	0.52	$4d_{z^2}$(Mo)	25	$p_z(C_h)$	25	p_z(Mo)	15
29*a* HOMO	−2.89	$4d_{yz}$(Mo)	46	$p_x(O_a)$	9	$p_x(C_a)$	9
28*b*	−2.93	$4d_{x^2-y^2}$(Mo)	33	$4d_{z^2}$(Mo)	19	$p_y(C_a)$	9
27*b*	−3.27	$4d_{xy}$(Mo)	33	$4d_{xy}$(Mo)	14	$p_x(O_a)$	9
28*a*	−3.31	$4d_{x^2-y^2}$(Mo)	17	$4d_{z^2}$(Mo)	16	$4d_{xy}$(Mo)	10
26*b*	−3.63	$4d_{x^2-y^2}$(Mo)	27	$p_x(C_h)$	23	$4d_{xy}$(Mo)	15
27*a*	−3.70	$4d_{xz}$(Mo)	15	$4d_{xy}$(Mo)	15	$4d_{z^2}$	9
26*a*	−7.18	*s*(H)	66	p_z(Mo)	10	$4d_{z^2}$(Mo)	6

molybdenum, nickel and iron complexes. This indicates that the stabilities of the Mo–H–Mo and Ni–H–Ni bonds in the known $[(CO)_5Mo–H–Mo(CO)_5]^-$ and $[(CO)_3Ni–H–Ni(CO)_3]^-$ complexes and in the hypothetical $[(CO)_4Fe–H–Fe(CO)_4]^-$ complex are comparable. On the other hand, the stability of the

TABLE 7

ENERGIES AND COMPOSITIONS OF HIGHEST OCCUPIED MOLECULAR LEVELS OF $[(CO)_4Fe–H–Fe(CO)_4]^-$ WITH D_{3h} SYMMETRY

MO	Energy (eV)	Largest contributions of the valence atomic orbitals (%)					
9*a*″ LUMO	−2.99	$3d_{z^2}$(Fe)	47	p_z(Fe)	24	$p_y(O_h)$	10
8*e*′ HOMO	−4.59	$3d_{xy}$(Fe) [a] $3d_{x^2-y^2}$	47	p_x(Fe) [a] p_y	14	$p_x(O_h)$	14
8*e*″	−4.69	$3d_{xy}$(Fe) [a] $3d_{x^2-y^2}$	48	p_x(Fe) [a] p_y	13	$p_x(O_h)$	13
7*e*″	−5.67	$3d_{xz}$(Fe) [a] $3d_{yz}$	65	$p_x(O_a)$ [a] p_y	8	$p_y(O_h)$	8
7*e*′	−5.72	$3d_{xz}$(Fe) [a] $3d_{yz}$	65	$p_v(O_h)$	9	$p_x(C_a)$ [a] p_y	9
$8a_1'$	−8.64	*s*H	52	p_z(Fe)	20	$3d_{z^2}$(Fe)	17
$7a_1'$	−12.53	$3d_{z^2}$(Fe)	35	$p_z(C_h)$	13	$p_z(O_h)$	10
$8a_2''$	−12.92	$3d_{z^2}$(Fe)	26	$p_z(C_a)$	11	$p_z(C_h)$	10
6*e*′	−13.35	$p_z(O_a)$	28	$p_z(C_a)$	24	p_x(Fe) [a] p_y	14
6*e*″	−13.37	$p_z(O_a)$	30	$p_z(C_a)$	24	p_x(Fe) [a] p_y	15
7*a*″	−14.84	$p_z(O_h)$	27	$p_y(O_h)$	25	$p_z(C_h)$	12
$6a_1'$	−15.04	$p_z(O_h)$	30	$p_y(O_h)$	16	$p_z(C_h)$	12
5*e*″	−15.16	$p_y(O_h)$	60	$p_y(C_h)$	26	$p_x(O_a)$ [a] p_y	9
$1a_1''$	−15.24	$p_x(O_h)$	69	$p_x(C_h)$	31		
$1a_2'$	−15.25	$p_x(O_h)$	69	$p_x(C_h)$	31		
5*e*′	−15.32	$p_y(O_h)$	52	$p_y(C_h)$	25	$p_x(O_a)$ [a] p_y	11

[a] Doubly degenerated molecular level.

TABLE 8

ENERGIES AND COMPOSITIONS OF HIGHEST OCCUPIED MOLECULAR LEVELS OF $[(CO)_3Ni–H–Ni(CO)_3]^-$ WITH D_{3h} SYMMETRY

MO	Energy (eV)	Largest contributions of the valence atomic orbitals (%)					
$6a_2''$ LUMO	0.61	p_y(C)	41	p_z(Ni)	28	p_y(O)	22
$6a_1'$ HOMO	−2.01	$3d_{z^2}$(Ni)	42	p_y(C)	19	p_z(Ni)	14
$7e'$	−2.33	$3d_{xz}$(Ni) [a] $3d_{yz}$	34	$3d_{xy}$(Ni) [a] $3d_{x^2-y^2}$	33	p_x(Ni) [a] p_y	11
$7e''$	−2.39	$3d_{xz}$(Ni) [a] $3d_{yz}$	34	$3d_{xy}$(Ni) [a] $3d_{x^2-y^2}$	33	p_x(Ni) [a] p_y	11
$5a_2''$	−3.07	$3d_{z^2}$(Ni)	90	p_yC	4	p_y(O)	3
$6e''$	−3.58	$3d_{xz}$(Ni) [a] $3d_{yz}$	53	$3d_{xy}$(Ni) [a] $3d_{x^2-y^2}$	32	p_x(C)	4
$6e'$	−3.60	$3d_{xz}$(Ni) [a] $3d_{yz}$	53	$3d_{xy}$(Ni) [a] $3d_{x^2-y^2}$	32	p_y(C)	4
$5a_1'$	−6.16	s(H)	57	$3d_{z^2}$(Ni)	35	p_z(Ni)	4
$5e'$	−11.13	p_z(C)	30	p_z(O)	19	p_x(Ni) [a] p_y	14
$5e''$	−11.20	p_z(C)	30	p_z(O)	19	p_x(Ni) [a] p_y	15
$4a_1'$	−13.52	p_z(O)	36	p_z(C)	32	s(Ni)	15
$4a_2''$	−13.59	p_z(O)	38	p_z(C)	31	s(Ni)	16
$1a_2'$	−14.94	p_x(O)	69	p_x(C)	31		
$1a_2''$	−14.94	p_x(O)	69	p_x(C)	31		
$4e'$	−15.02	p_y(O)	65	p_y(C)	32	p_x(O)	2
$4e''$	−15.03	p_y(O)	64	p_y(C)	31	p_x(O)	4

[a] Doubly degenerated molecular level.

Cr–H–Cr bond is somewhat lower (Table 10). One should emphasize that the stabilization energy of the last filled bridge orbital with respect to the HOMO energy as determined by us by the Fenske–Hall method for $(CH_3)_2Al\langle_{H}^{H}\rangle Al(CH_3)_2$

TABLE 9

ENERGIES AND COMPOSITIONS OF HIGHEST OCCUPIED MOLECULAR LEVELS OF $[(CO)_3Ni–H–Ni(CO)_3]^-$ WITH C_{2v} SYMMETRY

MO	Energy (eV)	Largest contributions of the valence atomic orbitals (%)					
$13b_1$ LUMO	1.31	p_z(Ni)	25	p_y(O)	23	p_y(O)	18
$13a_1$ HOMO	−1.39	$3d_{xz}$(Ni)	34	p_y(C)	21	p_z(Ni)	15
$8b_2$	−1.98	$3d_{xy}$(Ni)	50	$3d_{yz}$(Ni)	15	p_y(Ni)	10
$8a_2$	−1.98	$3d_{xy}$(Ni)	48	$3d_{yz}$(Ni)	21	p_y(Ni)	10
$12b_1$	−2.02	$3d_{xz}$(Ni)	45	$3d_{x^2-y^2}$(Ni)	18	p_x(Ni)	9
$12a_1$	−2.20	$3d_{z^2}$(Ni)	45	$3d_{x^2-y^2}$(Ni)	20	p_x(C)	8
$11b_1$	−2.44	$3d_{z^2}$(Ni)	74	$3d_{xz}$(Ni)	15	p_y(C)	3
$11a_1$	−3.01	$3d_{x^2-y^2}$(Ni)	46	$3d_{z^2}$(Ni)	27	$3d_{xz}$(Ni)	9
$7a_2$	−3.03	$3d_{yz}$Ni	69	$3d_{xy}$(Ni)	15	p_x(O)	3
$10b_1$	−3.06	$3d_{x^2-y^2}$(Ni)	52	$3d_{xz}$(Ni)	26	$3d_{z^2}$(Ni)	6
$7b_2$	−3.09	$3d_{yz}$(Ni)	71	$3d_{xy}$(Ni)	11	p_y(O)	5
$10a_1$	−5.68	s(H)	56	$3d_{xz}$(Ni)	25	$3d_{z^2}$(Ni)	10

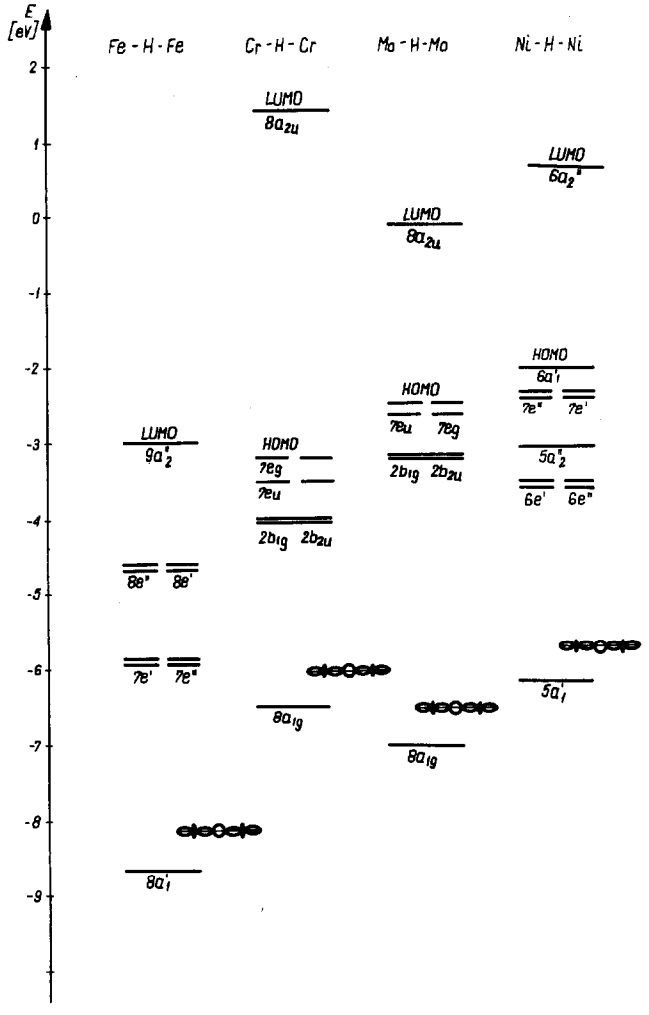

Fig. 6. Correlation of the molecular levels of the carbonyl dimers of Cr, Mo, Fe and Ni with linear single hydrogen bridges.

TABLE 10

STABILITY OF THE HYDROGEN BRIDGE

Compound	Symmetry	$\Delta E_{HOMO,MO(M-H-M)}$ (eV)	Ref.
$[(CO)_5Cr-H-Cr(CO)_5]^-$	D_{4h}	3.27	
$[(CO)_5Mo-H-Mo(CO)_5]^-$	D_{4h}	4.52	
$[(CO)_4Fe-H-Fe(CO)_4]^-$	D_{3h}	4.59	
$[(CO)_3Ni-H-Ni(CO)_3]^-$	D_{3h}	4.15	
$(CH_3)_2Al\begin{smallmatrix}H\\ \diamond\\ H\end{smallmatrix}Al(CH_3)_2$	D_{2h}	7.07	4

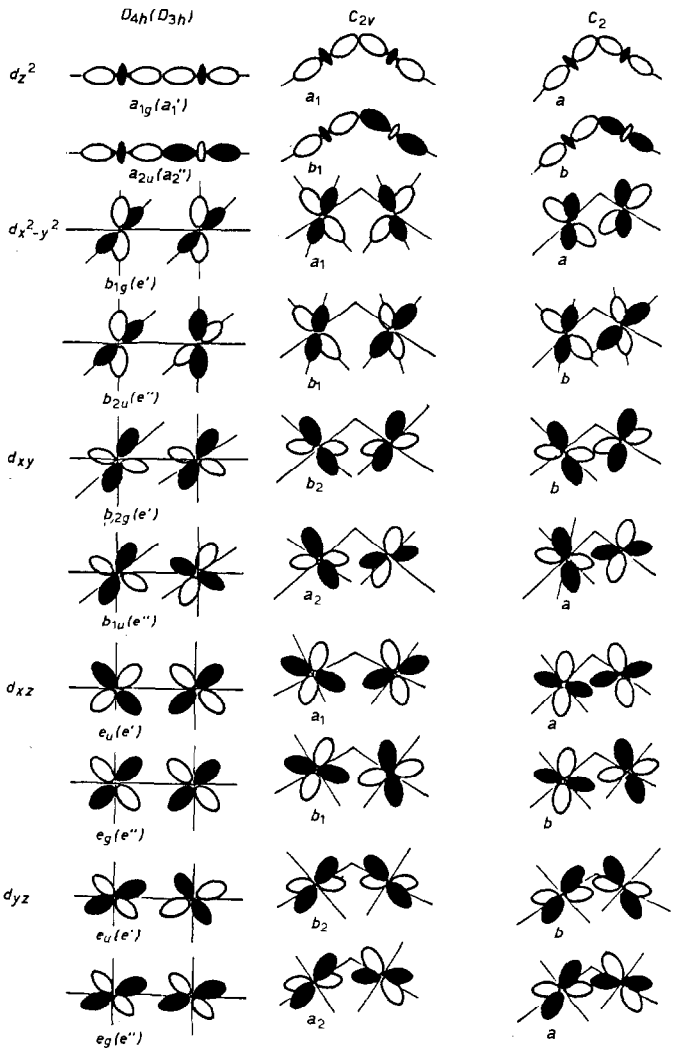

Fig. 7. Symmetry adapted linear combinations of the d atomic orbitals of the metal atoms.

is approximately twice as large as the values in the complexes discussed. This does not, however, result in a drastic difference in the stabilities of hydrogen bridges in $(CH_3)_2Al\langle^{H}_{H}\rangle Al(CH_3)_2$ and in carbonyl dimers.

For all the complexes with single hydrogen bridges discussed here, the group of last filled molecular orbitals corresponding to bonding interactions of the type $dM \rightarrow \pi^a(CO)$ provides the same contribution to the bonding and antibonding interactions between the metal atoms (Table 1, 4, 7, 9, Fig. 7). This is also reflected by the metal–metal (M–M) overlap population values (Table 11). For each complex the M–M overlap population is close to zero.

Thus, these complexes show no direct bonding between the metal atoms, this

takes place only through the hydrogen bridge as in $H_2B\langle^{H}_{H}\rangle BH_2$ and $(CH_3)_2Al\langle^{H}_{H}\rangle Al(CH_3)_2$. Slightly different metal–hydrogen (M–H) overlap populations for the Cr, Mo, Ni and Fe complexes shown in the Table 11 are indicative of the comparable covalent nature of the Cr–H–Cr, Mo–H–Mo, Ni–H–Ni, and Fe–H–Fe bonds. Furthermore, in $(CH_3)_2Al\langle^{H}_{H}\rangle Al(CH_3)_2$ the Al–H overlap population determined by the Fenske–Hall method is of the same order as that for the carbonyl complexes examined (Table 11).

The charges on the metal atoms vary from fairly large positive charges on the chromium and molybdenum atoms, a small negative charge on the nickel atom, to a fairly large negative charge on the iron atom (Table 12).

Since the bridging hydrogen atom is always provided with a negative charge, means that the Cr–H–Cr and Mo–H–Mo bonds are partly ionic, such as the Al–H–Al bond, however, the Ni–H–Ni and Fe–H–Fe bonds are exclusively covalent like the B–H–B bond.

One should also note that there is a very small negative charge on the bridging hydrogen atom in the iron complex of −0.050. This value differs considerably from the fairly large negative charges localized on the bridging hydrogen atom in chromium (−0.499), the molybdenum (−0.346) and nickel (−0.292) complexes (Table 12). Such a small negative charge on the bridging hydrogen atom in $[(CO)_4Fe–H–Fe(CO)_4]^-$ complex seems to be characteristic of the iron complexes since an equally low value (−0.080) was calculated by us for the $[(CO)_3Fe\langle^{H}_{CO}\rangle Fe(CO)_3]^-$ complex [16] of a known crystallographic structure.

Analysis of the electron density distribution for terminal ligands shows that in

TABLE 11

MULLIKEN OVERLAP POPULATIONS

Compound	Symmetry	Overlap populations						
		M–M	M–H	dM–H	M–C_h	M–C_a	dM–C_h	dM–C_a
$[(CO)_5Cr–H–Cr(CO)_5]^-$	D_{4h}	−0.002	0.070	0.069	0.280	0.274	0.206	0.241
	C_{2v}	−0.007	0.067	0.066	0.280	0.256	0.203	0.226
	C_2	−0.006	0.067	0.066	0.282	0.256	0.206	0.227
$[(CO)_5Mo–H–Mo(CO)_5]^-$	D_{4h}	0.006	0.149	0.059	0.365	0.355	0.209	0.231
	C_{2v}	−0.103	0.139	0.052	0.384	0.378	0.204	0.262
	C_2	−0.015	0.138	0.053	0.365	0.373	0.204	0.267
$[(CO)_4Fe–H–Fe(CO)_4]^-$	D_{3h}	0.003	0.161	0.054	0.375	0.399	0.180	0.194
$[(CO)_3Ni–H–Ni(CO)_3]^-$	D_{3h}	−0.025	0.114	0.036	0.411	0.099		
	C_{2v}	0.039	0.104	0.025	0.401	0.104		
		Al–Al	Al–H		Al–C			
$(CH_3)_2Al\langle^{H}_{H}\rangle Al(CH_3)_2$	D_{2h}	0.074	0.150		0.162			
Ref. [4]								

TABLE 12

MULLIKEN ATOMIC CHARGES

Compounds	Symmetry	Atomic charges			
		M	H	CO_h	CO_a
$[(CO)_5Cr-H-Cr(CO)_5]^-$	D_{4h}	0.596	−0.499	−0.153	−0.233
	C_{2v}	0.603	−0.491	−0.163	−0.204
	C_2	0.595	−0.497	−0.159	−0.209
$[(CO)_5Mo-H-Mo(CO)_5]^-$	D_{4h}	0.146	−0.346	−0.080	−0.155
	C_{2v}	0.344	−0.358	−0.105	−0.249
	C_2	0.164	−0.347	−0.060	−0.253
$[(CO)_4Fe-H-Fe(CO)_4]^-$	D_{3h}	−0.841	−0.050	0.088	0.103
$[(CO)_3Ni-H-Ni(CO)_3]^-$	D_{3h}	−0.024	−0.292	−0.110	
	C_{2v}	0.039	−0.336	−0.139	
$(CH_3)_2Al(\overset{H}{\underset{H}{\diamond}})Al(CH_3)_2$	D_{2h}	Al	H	CH_3	
(Ref. 4)		1.837	−0.506	0.135	

the chromium, molybdenum and nickel complexes the charges localized on the carbonyl groups are negative which indicates that the $d\mathrm{M} \rightarrow \pi^a(\mathrm{CO})$ interaction is a predominant contribution to the metal–carbonyl group bond (M–CO) (Table 13). With the same $M-CO_a$ and $M-CO_h$ distance assumed for calculations in the chromium and molybdenum complexes, larger negative charges on the CO_a groups than on the CO_h groups indicate that the $d\mathrm{M} \rightarrow \pi^a(\mathrm{CO_a})$ interaction is stronger than that for $d\mathrm{M} \rightarrow \pi^a(\mathrm{CO_h})$. A stronger interaction between the metal atoms and the CO_a groups should lead to shorter $M-CO_a$ bonds with respect to the $M-CO_h$ bonds a feature which is in fact observed in all crystallographically determined structures of $[(CO)_5M-H-M(CO)_5]^-$ anions.

Furthermore, it results in an increased lability of the CO_h groups if compared to the CO_a groups as shown experimentally [10c,10f,11,12,13]. Thus the cis effect of the bridging hydrogen atom found experimentally, was confirmed by our calculations.

We think that the stronger bonding of the CO_a groups to the complex might be a consequence of their participation in the formation of the bridge molecular orbital.

The $M-C_a$ and $M-C_h$ overlap population values which are almost the same for a given complex, indicate that the contribution of the covalent effect in the metal–carbonyl bond does not depend on the position of the carbonyl group (Table 11). It is noteworthy that in the Cr–CO and Mo–CO bonds the main covalent contribution is provided by the *d* orbitals of the metal atoms, in the Ni–CO bond, however, this is provided by the *s* and *p* orbitals of the metal atoms as indicated by the values of the respective overlap populations (Table 11). But in the Fe–CO bond the covalent contributions of the *d* as well as the *s* and *p* orbitals of the metal atoms are similar.

In contrast to other complexes discussed a positive charge is localized on the terminal ligands in $[(CO)_4Fe-H-Fe(CO)_4]^-$ (Table 12). This means a higher contribution by CO–M interactions than $d\mathrm{M} \rightarrow \pi^a(\mathrm{CO})$ to the Fe–CO bond.

2. Influence of the hydrogen bridge geometry and mutual orientation of the mononuclear fragments on the electronic structure of the $[(CO)_3Ni–H–Ni(CO)_3]^-$ and $[(CO)_5M–H–M(CO)_5]^-$ anions.

For $[(CO)_3Ni–H–Ni(CO)_3]^-$ a transition from the linear to the bent hydrogen bridge with retention of the eclipsed conformation results in practically no changes in energy of the lower filled energy levels, i.e. those mainly having σMO and Π^bMO character of the CO groups or correspond to σCO–M interactions.

On the other hand, the level corresponding to the M–H–M bond and those corresponding to the $d_{xz} \rightarrow \Pi^a$(CO) interactions, i.e. $6e'$, $6e''$; $7e'$ and $7e''$ increase by 0.5 eV (Fig. 8). This results from participation of the $3d_{xz}$Ni orbitals in the bridge bond in an anion with C_{2v} symmetry. The qualitative composition of the HOMO orbital also undergoes changes. The $6a_1$ orbital which is the highest filled orbital for the $[(CO)_3Ni–H–Ni(CO)_3]^-$ anion of D_{3h} symmetry and is formed to a fairly large extent by the $3d_{z^2}$Ni orbitals, is replaced by the $13a_1$ orbital, which, in turn, consists mainly of $3d_{xz}$Ni orbitals (Table 8).

Since we are comparing chemically identical systems differing only in their symmetries, the energy of the HOMO orbital may be assumed to be an approximate measure of the total energy of the system. Therefore, the conformation with the linear bridge with D_{4h} symmetry is slightly more favourable, from an energetic point of view, to that with a bent bridge with C_{2v} symmetry.

Moreover, stabilization of the bridge molecular orbital with respect to the HOMO orbital remains practically unchanged. No large changes occur in the

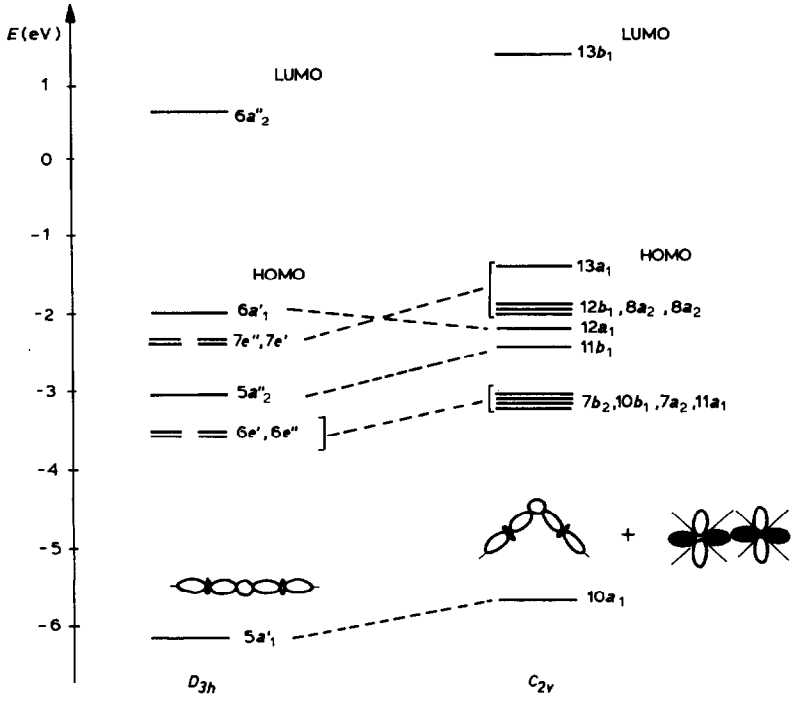

Fig. 8. Influence of lowering the symmetry of the complex on the electronic structure of $[(CO)_3Ni–H–Ni(CO)_3]^-$.

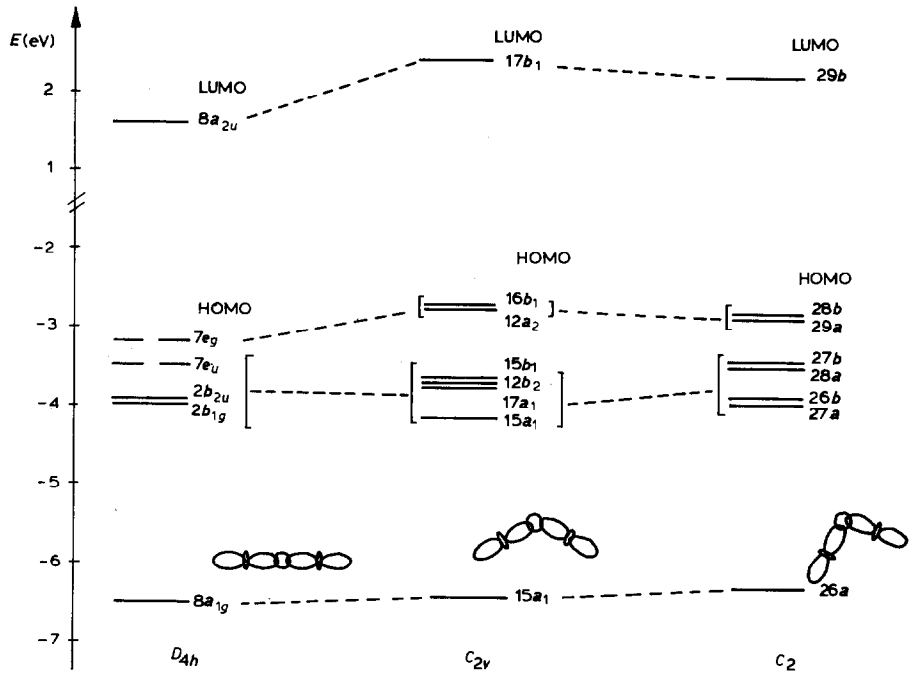

Fig. 9. Influence of lowering the symmetry of the complex on the electronic structure of $[(CO)_5Cr–H–Cr(CO)_5]^-$.

electron density distribution in the complex (Table 11, 12). However, after bending the bridge, the Ni–H–Ni bond character becomes ionic to a slight extent, since small negative charges on the metal atoms, for D_{3h} symmetry, are changed into small positive charges, for C_{2v} symmetry (Table 12).

Changes in the electronic structure of the $[(CO)_5Cr–H–Cr(CO)_5]^-$ anion are a result of the linear hydrogen bridge bending so that the Cr–H–Cr angle is 145° and mutual shifting of the mononuclear fragments by 20° is due to the last filled levels corresponding to the $dCr \rightarrow \pi^a(CO)$ interactions (Table 2, 3). These changes are the result of the mixing of the $3d$ orbitals of the chromium atoms. This is presumed to be due to the combination of the d_{z^2}, $d_{x^2-y^2}$, d_{xz} orbitals, or d_{xy} and d_{yz} orbitals for the anion with C_{2v} symmetry and the combination of all five d orbitals for the anion with C_2 symmetry (Fig. 7).

Figure 9 shows the correlation of the last filled molecular orbital for the anion, $[(CO)_5Cr–H–Cr(CO)_5]^-$, with D_{4h}, C_{2v} and C_2 symmetries. The bridge molecular orbital $8a_1$ in the linear bridge system is transformed, on lowering the complex symmetry to C_{2v} and to C_2, into the $15a_1$ and $26a$ orbitals, respectively.

As shown in Tables 2 and 3 and in Fig. 9 lowering the anion symmetry has very little effect on the percentage composition of the bridge orbital and so its energy remains practically unchanged. One can thus assume that any change in anion symmetry has no effect on the structure and energy of the bridge orbital. On the other hand, the energy of the HOMO orbital on changing from the D_{4h} to C_{2v} symmetry is somewhat increased and then, on lowering the symmetry to C_2, it decreases slightly. Changes in the qualitative composition of the HOMO orbital are

also characteristic. The $7e_g$ orbital which is a HOMO orbital for the system with D_{4h} symmetry consists, for about 60%, of the $3d_{xz}$ and $3d_{yz}$ orbitals of the Cr atoms whereas for its C_{2v} symmetry, the $12a_2$ and $16b_1$ orbitals also contain a slight $3d_{xy}$ and $3d_{z^2}$ contribution (Tables 2 and 3). For the C_2 symmetry the qualitative composition of the last filled $29a$ and $28b$ orbitals again corresponds to that of the $7e_g$ orbital in the complex with D_{4h} symmetry. It is also worth mentioning that there is slight but characteristic effect of reducing the symmetry on the lower energy levels the nature of which corresponds mainly to the terminal ligand orbitals. The levels with exclusively σCO or π^b(CO) character for the D_{4h} symmetry become delocalized. For C_{2v} or C_2 symmetry these levels are simultaneously of σ and π^b character. Furthermore, the levels of the π^b character become destabilized to a slight extent.

Here we emphasize, however, that with such relatively slight deviations from D_{4h} symmetry, which was allowed for in the calculations for the chromium complex, there are no definite energy preferences for any of the three conformations with the D_{4h}, C_{2v} and C_2 symmetries.

As indicated by the results of population analysis presented in Tables 11, 12 there are also no essential changes in the electron density distribution in the complex on transition from a linear hydrogen bridge for D_{4h} symmetry to a bent bridge for C_{2v} and C_2 symmetries.

The Cr–Cr overlap population, moreover, in spite of a slightly shorter distance between the metal atoms, undergoes practically no changes. For each one of the three conformations the atomic orbitals of the metal contribute in equal amounts to the formation of bonding and antibonding molecular orbitals (with respect to the M–M axis) (Table 1, 2 and 3). Thus, regardless of the $[(CO)_5Cr–H–Cr(CO)_5]^-$ complex symmetry, the bond between the metal atoms occurs exclusively through the hydrogen bridge. It would seem, therefore, that the M–H–M bond in the $[(CO)_5M–H–M(CO)_5]^-$ anions is "flexible", permitting a change in the system symmetry, e.g. under the influence of the crystal lattice, without any substantial changes in density distribution in the system or in its energy.

However, as shown by comparison of the electronic structure of $[(CO)_5Mo–H–Mo(CO)_5]^-$ which also has D_{4h}, C_{2v} and C_2 symmetries (Table 4, 5, 6) but with a smaller M–H–M angle than that of the chromium complex discussed previously, the flexibility of the M–H–M bond has certain limitations. When the M–H–M angle for the molybdenum complex is 127° and the mononuclear $M(CO)_5$ fragments are in the eclipsed position, destabilization of the two molecular levels having π^bCO_h character is so high that they become the last filled molecular levels $16b_1$ and $12a_2$ (Fig. 10). This is probably as a result of strong antibonding interactions between the π^bMOs of proximal CO_h groups, derived from various fragments of $Mo(CO)_5$.

In effect, the energy of the HOMO level for C_{2v} symmetry is much higher than that of the HOMO level for D_{4h} symmetry. The energy difference between the LUMO and HOMO orbitals decreased considerably. Thus, after bending of the bridge the entire system is markedly less stable. These energy effects are unfavourable for complex stability and are a result of the large bend of the hydrogen bridge being eliminated on changing to the C_2 symmetry as shown in Fig. 10. Owing to a 45° shift of the mononuclear fragments to form a staggered conformation, the molecular orbitals of the $\pi^b(CO_h)$ character restabilize. Thus, the HOMO energy was reduced to a somewhat lower value than that of the HOMO energy in the

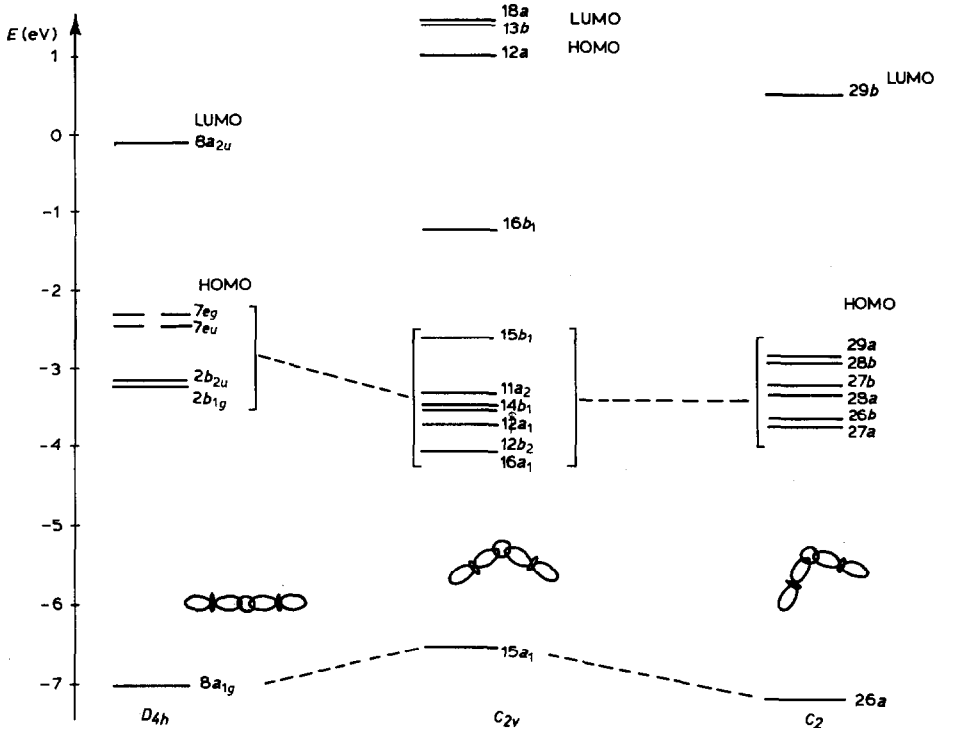

Fig. 10. Influence of lowering the symmetry of the complex on the electronic structure of $[(CO)_5Mo–H–Mo(CO)_5]^-$.

system having the D_{4h} symmetry. Taking into account the energy values of the HOMO level and the gap between LUMO and HOMO one finds that the stabilities of the $[(CO)_5Mo–H–Mo(CO)_5]^-$ complex in the C_2 and D_{4h} symmetries are comparable. Moreover the results of the population analysis indicate that the least favourable conformation for the molybdenum anion is one with C_{2v} symmetry. For the D_{4h} and C_2 symmetries the electron density distribution in the complex is almost identical (Tables 11 and 12).

The Mo–Mo overlap populations in both systems are close to zero which shows that there are no direct bonding or antibonding interactions between the metal atoms (Table 11). On the other hand, for the C_{2v} symmetry the Mo–Mo overlap population has a fairly large negative value (-0.103) which is indicative of direct antibonding interactions between the metal atoms.

One should also emphasize here that for the $[(CO)_5Mo–H–Mo(CO)_5]^-$ complex a transition from D_{4h} to C_{2v} and C_2 symmetries does not result in any essential changes in the energy and composition of the bridge orbital or in the magnitude of the charge localized on the hydrogen atom and magnitude of the M–H overlap population (Tables 10 and 11).

Conclusions

In the present paper we have found that there is no direct M–M bond in the chromium, molybdenum, iron and nickel carbonyl dimers with single hydrogen

bonds. The metal atoms are bonded exclusively through the hydrogen bridge. The 1*s* atomic orbital of the bridging hydrogen atom is poorly delocalized providing a significant contribution to the formation of only one filled molecular orbital corresponding to the M–H–M bond. The hydrogen bridge stability for the Mo, Ni, Fe complexes is similar but in the chromium complex it is somewhat diminished.

The covalent character of the bridge bond is the same for all the complexes discussed here however, ionic character depends on the type of metal since the charge on the hydrogen atom is always negative in these complexes.

We have found that the M–H–M bond can in fact be described as flexible in the case of carbonyl dimers with single hydrogen bridges. This is because the M–H–M angle may vary in such complexes over fairly broad ranges without substantial changes in the electronic structure of the complex and hydrogen bridge stability.

Even when a bridge deflection is too large and unfavourable energy changes occur in the electronic structure of the complex reducing its stability, the system then assumes a staggered conformation which removes unfavourable effects. In the $[(CO)_5M–H–M(CO)_5]^-$ complexes, the *cis* effect of the bridging hydrogen atom found experimentally, was confirmed by our calculations.

In general, on the grounds of our calculations one can say that for both the electronic structure and its nature, the metal–hydrogen–metal bridge bond in the carbonyl complexes of transition metals with single hydrogen bridges does not essentially differ from the bridge bonds B–H–B and Al–H–Al and so belongs to the same family of bonds although it is much less stable.

Other aspects of the M–H–M bridge bond will be discussed in future papers.

Acknowledgement

This work was financially supported by the Project No. M.R.I.9 of Polish Academy of Sciences.

References

1 (a) R. Bau, R.G. Teller and S.W. Kirtley, Acc. Chem. Res., 12 (1976) 176. (b) R. Bau and T.F. Koetzle, Pure Appl. Chem., 50 (1978) 55. (c) R. Bau, P. Gütlich and R.G. Teller, Structure and Bonding, 44 (1981) 3.

2 (a) E.A. Laws, R.M. Stevens and W.N. Lipscomb, J. Am. Chem. Soc., 94 (1972) 4461. (b) I.R. Epstein, D. Marynick and W.N. Lipscomb, J. Am. Chem. Soc., 95 (1973) 1760. (c) T.E. Taylor and M.B. Hall, J. Am. Chem. Soc., 102 (1980) 6136.

3 M. Pelissier and J.P. Malrieu, Theoret. Chim. Acta, 56 (1980) 175.

4 B. Jeżowska-Trzebiatowska and B. Nissen-Sobocińska; manuscript in preparation

5 R.G. Hayter, J. Am. Chem. Soc., 89 (1966) 4376.

6 G. Longoni, M. Manassero and M. Sansoni, J. Organomet. Chem., 174 (1979) C41.

7 K.S. Wong, W.R. Scheidt and J.A. Labinger, Inorg. Chem., 18 (1976) 136.

8 L.B. Handy, P.M. Treichel, L.F. Dahl and R.G. Hayter, J. Am. Chem. Soc., 88 (1966) 366.

9 L.B. Handy, J.K. Ruff and L.F. Dahl, J. Am. Chem. Soc., 92 (1970) 7312.

10 (a) J.P. Olsen, T.F. Koetzle, S.W. Kirtley, M. Andrews, D.L. Tipton and R. Bau, J. Am. Chem. Soc., 96 (1974) 6621. (b) R.D. Wilson, S.A. Graham and R. Bau, J. Organomet. Chem., 91 (1975) C49. (c) R.A. Love, H.B. Chin, T.F. Koetzle, S.W. Kirtley, B.R. Whittlesey and R. Bau, J. Am. Chem. Soc., 98 (1976) 4493. (d) J. Roziere, J.M. Williams, R.P. Stewart, J.L. Petersen and L.F. Dahl, J. Am. Chem. Soc., 99 (1977) 4497. (e) J.L. Petersen, P.L. Johnson, J. O'Connor, L.F. Dahl and J.M. Williams, Inorg. Chem., 17 (1978) 3460. (f) M.Y. Darensbourg, J.L. Atwood, R.R. Burch, W.E. Hunter and N.

Walker, J. Am. Chem. Soc., 101 (1979) 2633. (g) J.L. Petersen, R.K. Brown, J.M. Williams and R.K. McMullan, Inorg. Chem., 18 (1979) 3493. (h) J.L. Petersen, R.K. Brown and J.M. Williams, Inorg. Chem., 20 (1981) 158. (i) J.L. Petersen, A. Masino and R.P. Stewart, J. Organomet. Chem., 208 (1981) 55. (j) J. Roziere, P. Teulon and M.D. Grillone, J. Am. Chem. Soc., 22 (1983) 557.
11 M.Y. Darensbourg and N. Walker, J. Organomet. Chem., 117 (1976) C68.
12 M.Y. Darensbourg, N. Walker and R.R. Burch, J. Am. Chem. Soc., 17 (1978) 52.
13 D.J. Darensbourg and M.J. Incorvia, Inorg. Chem., 18 (1979) 18.
14 C.B. Cooper III, D.F. Shriver and S. Onaka, Adv. Chem. Ser., 167 (1978) 232.
15 M.B. Hall and R.F. Fenske, Inorg. Chem., 11 (1972) 768.
16 B. Jeżowska-Trzebiatowska and B. Nissen-Sobocińska; manuscript in preparation